

Exceptional high-strain-rate superplasticity in Mg–Gd–Y–Zn–Zr alloy with long-period stacking ordered phase

Q. Yang,^a B.L. Xiao,^a Q. Zhang,^a M.Y. Zheng^b and Z.Y. Ma^{a,*}

^aShenyang National Laboratory for Materials Science, Institute of Metal Research, Chinese Academy of Sciences, 72 Wenhua Road, Shenyang 110016, People's Republic of China

^bSchool of Materials Science and Engineering, Harbin Institute of Technology, 92 West Dazhi Street, Harbin 150001, People's Republic of China

Received 13 August 2013; revised 3 September 2013; accepted 3 September 2013
Available online 8 September 2013

Friction stir processing (FSP) was applied to Mg–Gd–Y–Zn–Zr casting, producing a fine-grained structure of $\sim 3 \mu\text{m}$ with a long-period stacking ordered phase distributed within the grains and predominantly high-angle grain boundaries. This FSP alloy exhibited superior high-strain-rate superplasticity at 350–500 °C. A maximum superplasticity of 3570% was achieved at 425 °C and a strain rate of $3 \times 10^{-2} \text{ s}^{-1}$. Such superior superplasticity is attributed to the thermally stable microstructure and good deformation compatibility.

© 2013 Acta Materialia Inc. Published by Elsevier Ltd. All rights reserved.

Keywords: Magnesium alloys; Long-period stacking ordered structure; Friction stir processing; Superplasticity

Mg–Zn–RE (rare earth) alloys with long-period stacking ordered (LPSO) phases have attracted much attention in recent years, due not only to their superior mechanical properties, but also to the special structure of the LPSO phase [1–4]. Studies revealed that the Mg–Zn–RE alloys are highly suited to plastic deformation such as extrusion and rolling [2,5–7], and exhibit high strength at both room and elevated temperatures due to the thermally stable LPSO phase. Therefore, the Mg–Zn–RE alloys possess potential for developing wrought products. For broader engineering applications, the ability to form magnesium alloys readily is necessary in order to fabricate complicated components. Superplastic forming is a promising method for achieving this goal.

In general, superplasticity can be obtained in materials with thermally stable fine grains ($< 10 \mu\text{m}$). It is thus believed that Mg–Zn–RE alloys with a LPSO phase should exhibit superior superplasticity, since the grains can be refined to $< 10 \mu\text{m}$ and the thermally stable LPSO phase can suppress grain growth at high temperatures [2,4]. However, reports on the superplasticity of Mg–Zn–RE alloys have so far been limited. Kawamura

et al. [1] first reported a high superplasticity of 780% at 350 °C and a high strain rate of $6 \times 10^{-2} \text{ s}^{-1}$ in a rapidly solidified powder metallurgy (RS P/M) processed $\text{Mg}_{97}\text{Zn}_1\text{Y}_2$ alloy. Wu et al. [8] obtained a superplasticity of 495% at 450 °C and $1.67 \times 10^{-3} \text{ s}^{-1}$ in an extruded $\text{Mg}_{96.32}\text{Gd}_{2.5}\text{Zn}_1\text{Zr}_{0.18}$ alloy. Recently, Leng et al. [9] achieved a superplasticity of 720% at 420 °C and $1 \times 10^{-3} \text{ s}^{-1}$ in an extruded Mg–9RY–4Zn (RY: Y-rich misc metal) alloy.

From the above findings, it is clear that the optimum superplasticity and the optimum strain rate for Mg–Zn–RE alloys are generally lower than those for other magnesium alloys [10–12]. This difference can be attributed to the fact that neither the superplastic deformation condition nor the microstructure was optimized in the studied Mg–Zn–RE alloys. The optimum deformation condition was not explored in the RS P/M $\text{Mg}_{97}\text{Zn}_1\text{Y}_2$ alloy, and the inhomogeneous microstructure of the extruded $\text{Mg}_{96.32}\text{Gd}_{2.5}\text{Zn}_1\text{Zr}_{0.18}$ and Mg–9RY–4Zn alloys caused cavitation in the LPSO/Mg interface during superplastic deformation, thereby resulting in early failure [1,8,9]. Therefore, if a uniform and fine-grained microstructure can be produced in the Mg–Zn–RE alloys, achieving enhanced superplasticity should be possible.

In our recent study, a uniform and fine-grained microstructure with the LPSO phase only within the

*Corresponding author. Tel./fax: +86 24 83978908; e-mail: zyma@imr.ac.cn

grains was produced in Mg–Gd–Y–Zn–Zr casting by friction stir processing (FSP) [13]. It is expected that such fine-grained structure would exhibit excellent superplasticity. In this study, superplasticity of the FSP Mg–Gd–Y–Zn–Zr alloy was investigated. It is indicated that an exceptionally high superplasticity of 3570% was obtained at 425 °C and a high strain rate of $3 \times 10^{-2} \text{ s}^{-1}$.

A 6 mm thick Mg–9.4Gd–4.1Y–1.2Zn–0.4Zr (wt.%) cast plate was subjected to single-pass FSP at a rotation rate of 800 rpm and a transverse speed of 100 mm min^{-1} . A tool with a concave shoulder 20 mm in diameter and a threaded conical pin 8 mm in root diameter and 4.6 mm in length was used. Microstructural characterization was performed on the cross-section of the stir zone (SZ) by optical and transmission electron microscopy (OM and TEM; Tecnai F20). Electron backscatter diffraction (EBSD) orientation maps were obtained using a Zeiss Supra 35. Specimens for EBSD observation were electropolished in a solution consisting of 60 ml nitric acid and 140 ml ethanol, followed by ion milling.

Mini tensile specimens (2.5 mm gage length, 1.4 mm gage width and 0.8 mm gage thickness) were machined perpendicular to the FSP direction, with the gage length centered in the SZ. Each specimen was fastened in the tensile testing apparatus as the furnace was heated to the selected testing temperature, and then held at this temperature for 20 min to establish thermal equilibrium prior to the tensile test. Tensile tests were conducted at a constant crosshead speed using an Instron 5848 microtester.

The microstructure of the FSP Mg–Gd–Y–Zn–Zr alloy is shown in Figure 1. The OM image reveals uniform and fine grains of $\sim 3 \mu\text{m}$, within which fine lamellae were clearly observed (Fig. 1a). The TEM image shows that no grain boundary particles were observed, and the fine lamellae with a width ranging from ~ 50 to $\sim 100 \text{ nm}$ were distributed throughout the grains (Fig. 1b). The fine lamellae were identified to be the LPSO phase by selected-area electron diffraction (SAED) patterns, as reported previously [13].

Figure 1c shows the microstructure of the FSP Mg–Gd–Y–Zn–Zr alloy obtained by EBSD mapping.

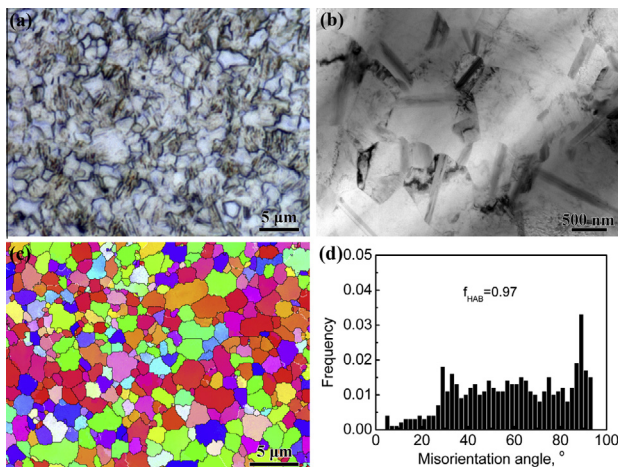


Figure 1. (a) OM and (b) TEM micrographs; (c) EBSD map and (d) boundary misorientation distribution of the FSP Mg–Gd–Y–Zn–Zr alloy.

High-angle grain boundaries (HAGBs, grain boundary misorientations $\geq 15^\circ$) and low-angle grain boundaries (grain boundary misorientations $< 15^\circ$) are shown by black and white lines, respectively. The microstructure was characterized by equiaxed grains with predominantly HAGBs. The fraction of the HAGBs was determined to be 97% (Fig. 1d).

Figure 2a shows the variation of elongation with initial strain rate for the FSP Mg–Gd–Y–Zn–Zr alloy at 400 and 425 °C. Exceptionally high superplasticity was observed at high strain rates. At strain rates of 1×10^{-2} – $3 \times 10^{-1} \text{ s}^{-1}$, elongations of $>1000\%$ were achieved at both temperatures. The optimum strain rate at both temperatures was $3 \times 10^{-2} \text{ s}^{-1}$, and the optimum superplasticity was above 3300% at both temperatures. A maximum elongation of 3570% was achieved at 425 °C.

Figure 2b shows the effect of temperature on the superplastic elongation for the FSP Mg–Gd–Y–Zn–Zr alloy at an initial strain rate of $3 \times 10^{-2} \text{ s}^{-1}$. The FSP alloy exhibited high-strain-rate superplasticity (HSRSP) of $>800\%$ over a wide temperature range of 350–500 °C. The optimum temperature was determined to be 425 °C. Therefore, a maximum superplasticity of 3570% was achieved at 425 °C and a high strain rate of $3 \times 10^{-2} \text{ s}^{-1}$.

For comparison, superplastic data for various magnesium alloys prepared via a variety of processing methods are summarized in Table 1. It is evident that, although the grain size in the present FSP Mg–Gd–Y–Zn–Zr alloy is relatively large compared with most superplastic magnesium alloys, the superplasticity in the FSP Mg–Gd–Y–Zn–Zr alloy is the highest among the investigated magnesium alloys.

The variation of flow stress (at a true strain of 0.1) with initial strain rate for the FSP Mg–Gd–Y–Zn–Zr alloy is shown in Figure 2c. The strain-rate sensitivity m is ~ 0.6 at both 400 and 425 °C for strain rates of 1×10^{-2} – $3 \times 10^{-1} \text{ s}^{-1}$. Such a high value of m indicates that the dominant deformation mechanism is grain boundary sliding (GBS) [14].

Figure 3 shows the appearance of tensile specimens deformed to failure at $3 \times 10^{-2} \text{ s}^{-1}$ at different temperatures. It is apparent that the deformed specimens exhibit

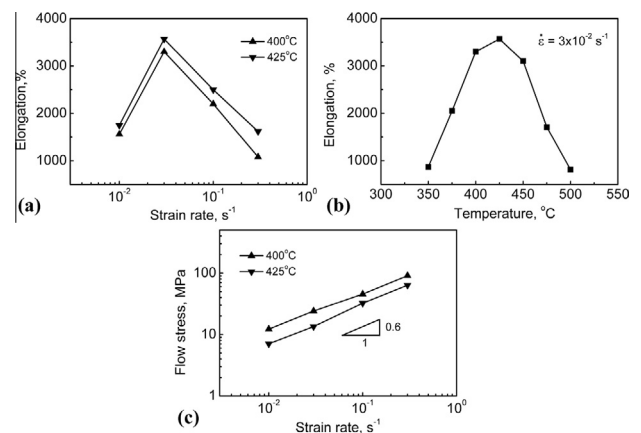


Figure 2. Variation of elongation with (a) initial strain rate and (b) temperature; (c) variation of flow stress with initial strain rate for the FSP Mg–Gd–Y–Zn–Zr alloy.

Table 1. A summary of optimum and/or high strain rate superplasticity in magnesium alloys.

Alloy	Processing	Grain size (μm)	Temperature ($^{\circ}\text{C}$)	Strain rate (s^{-1})	Elongation (%)	Refs.
ZK60	HRDSR ^a	1	280	1×10^{-2}	926	[20]
ZK60	ECAP ^b	0.8	200	1×10^{-4}	3050	[10]
AZ61	ECAP	0.6	200	3.3×10^{-4}	1320	[21]
AZ91	FSP	1.2	350	3×10^{-3}	1202	[22]
Mg–15Al–1Zn	Extrusion	3	325	1×10^{-2}	1610	[23]
Mg–8Al–8Ga	RS P/M	2	300	1×10^{-2}	1080	[12]
Mg–8Li	ECAP	2.5	200	1.5×10^{-4}	1780	[24]
Mg–7.1Zn–1.2Y–0.8Zr	FSP	4.5	450	1×10^{-2}	1110	[11]
Mg ₉₇ Zn ₁ Y ₂	RS P/M	0.1–0.15	350	6×10^{-2}	780	[1]
WE43	Extrusion	2	400	1×10^{-4}	1216	[25]
Mg–9.4Gd–4.1Y–1.2Zn–0.4Zr	FSP	3	425	3×10^{-2}	3570	Present work

^a High-ratio differential speed rolling.

^b Equal channel angular pressing.

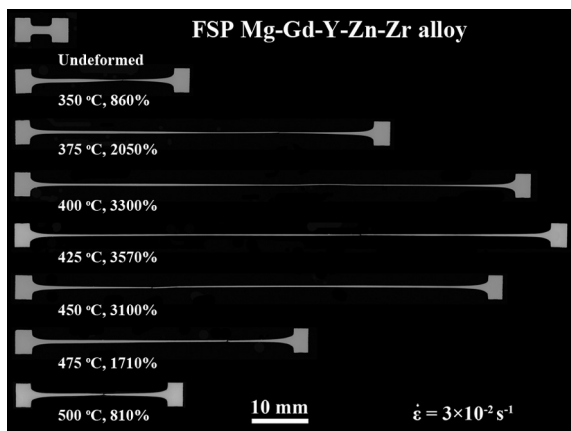


Figure 3. Tensile specimens pulled to failure at a strain rate of $3 \times 10^{-2} \text{ s}^{-1}$ for different temperatures.

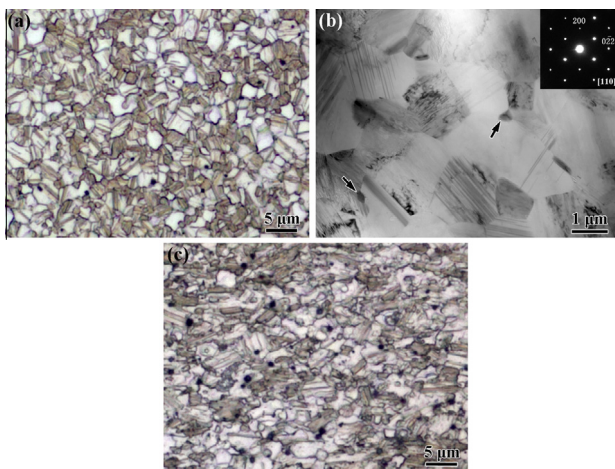


Figure 4. Microstructure of the FSP Mg–Gd–Y–Zn–Zr sample deformed at $425 \text{ }^{\circ}\text{C}$ and $3 \times 10^{-2} \text{ s}^{-1}$ to failure: (a) OM and (b) TEM images of the grip section; (c) OM image of the gage section.

the characteristics of superplastic deformation, with relatively uniform elongation.

Figure 4 shows the microstructure of the specimen deformed to failure at $425 \text{ }^{\circ}\text{C}$ and $3 \times 10^{-2} \text{ s}^{-1}$. As shown in **Figure 4a**, the grains in the grip section grew slightly from ~ 3 to $\sim 4 \mu\text{m}$ after static annealing for ~ 40 min, indicating high thermal stability of the FSP Mg–Gd–Y–Zn–Zr alloy. In addition, widening of the

LPSO lamellae could be clearly observed. The TEM image in **Figure 4b** further confirms the widening and enhanced precipitation of LPSO lamellae, indicating the growth and coagulation of the LPSO phase during annealing. Furthermore, a small number of fine particles with an average size of $\sim 300 \text{ nm}$ were observed at the grain boundaries, as indicated by the arrows in **Figure 4b**. These particles were identified from the SAED patterns as $\beta\text{-Mg}_5\text{Gd}$ -type compound. Energy-dispersive spectroscopy analyses showed that the average compositions of β particles were $\text{Mg-}9.9 \pm 0.2\text{Gd-}6.0 \pm 0.3\text{Y-}2 \pm 0.1\text{Zn}$ (at.%).

The precipitation of β particles was also observed in our previous study of the superplastic Mg–Gd–Y–Zr alloy, and was attributed to the supersaturated initial matrix [15]. However, the size and volume fraction of β particles in the FSP Mg–Gd–Y–Zn–Zr alloy were lower than those in Mg–Gd–Y–Zr alloy with similar alloy contents. This should be attributed to the addition of Zn in the FSP Mg–Gd–Y–Zn–Zr alloy. The study by Yamasaki et al. [16] suggested that addition of Zn to Mg–Gd alloys could promote the precipitation of LPSO phase and inhibit precipitation of the β phase during annealing at above $350 \text{ }^{\circ}\text{C}$. In this case, the LPSO lamellae precipitated preferentially in the FSP Mg–Gd–Y–Zn–Zr alloy during annealing at $425 \text{ }^{\circ}\text{C}$, whereas the precipitation of the β particles was suppressed.

Figure 4c shows the microstructure of the gage section after superplastic deformation. The grains grew slightly to $\sim 4.7 \mu\text{m}$ under dynamic loading, revealing high thermal stability. In addition, the grains remained equiaxed, confirming the dominant GBS mechanism. Widening of the LPSO lamellae was also observed, and no detectable kinking of the LPSO lamellae occurred. In addition, hardly any cavities were observed throughout the gage section region, indicating high deformation compatibility of the FSP Mg–Gd–Y–Zn–Zr alloy.

The superior HSRSP of the FSP Mg–Gd–Y–Zn–Zr alloy is attributed to its special microstructure. First, the FSP Mg–Gd–Y–Zn–Zr alloy had uniform and fine equiaxed grains, with LPSO lamellae being distributed throughout the grains. The thermally stable LPSO lamellae can act as a skeleton in the relatively soft grains. In this case, the grain boundary motion was inhibited by LPSO lamellae, and high thermal stability

of the grains was retained even at 425 °C. It is documented that increasing the temperature and decreasing the grain size contribute to achieving HSRSP [17]. Thus, HSRSP was achieved in the fine-grained FSP Mg–Gd–Y–Zn–Zr alloy at temperatures higher than that for conventional superplastic magnesium alloys. Furthermore, the uniform fine and equiaxed grains exhibited good deformation compatibility, and thus cavitation could be minimized during superplastic deformation, leading to large elongation to failure.

Second, the FSP Mg–Gd–Y–Zn–Zr alloy had a high percentage of HAGBs. The predominant HAGBs facilitated GBS and accelerated superplastic deformation kinetics [18]. Therefore, HSRSP was obtained.

Third, only a small number of fine grain boundary β particles precipitated during superplastic deformation. Although there is a good deformation compatibility between the LPSO particles and the matrix in the superplastic Mg–Zn–RE alloys with the grain boundary LPSO phase, cavities occurred at the interface between large LPSO particles and the matrix, resulting in a low superplasticity [8,9]. In the FSP Mg–Gd–Y–Zn–Zr alloy with fine LPSO lamellae distributed within the grains, no deformation incompatibility between the LPSO particles and the matrix was generated, leading to the suppression of cavitation. Moreover, a study by Li et al. [19] suggested that the β particles can deform during superplastic tension at 435 °C, thus part of the strain can be transformed from the matrix to the β particles. Therefore, a small number of fine grain boundary β particles precipitated during superplastic deformation in the FSP Mg–Gd–Y–Zn–Zr alloy contributed to releasing rather than generating stress concentration. In this case, the FSP Mg–Gd–Y–Zn–Zr alloy exhibited good deformation compatibility, and large superplastic elongation was achieved.

In summary, a FSP Mg–Gd–Y–Zn–Zr alloy with fine grains and LPSO phase distributed within the grains exhibited a superior HSRSP of 3570% at 425 °C and $3 \times 10^{-2} \text{ s}^{-1}$.

This work is supported by the National Natural Science Foundation of China under Grant Nos. 50901075 and 51331008.

[1] Y. Kawamura, K. Hayashi, A. Inoue, T. Masumoto, *Mater. Trans.* 41 (2001) 1172.

- [2] G. Bi, D. Fang, L. Zhao, J. Lian, Q. Jiang, Z. Jiang, *Mater. Sci. Eng. A* 528 (2011) 3609.
- [3] Y.M. Zhu, A.J. Morton, J.F. Nie, *Acta Mater.* 58 (2010) 2936.
- [4] K. Hagihara, A. Kinoshita, Y. Sugino, M. Yamasaki, Y. Kawamura, H.Y. Yasuda, Y. Umakoshi, *Acta Mater.* 58 (2010) 6282.
- [5] T. Itoi, K. Takahashi, H. Moriyama, M. Hirohashi, *Scripta Mater.* 59 (2008) 1155.
- [6] M. Yamasaki, T. Anan, S. Yoshimoto, Y. Kawamura, *Scripta Mater.* 53 (2005) 799.
- [7] C. Xu, M.Y. Zheng, S.W. Xu, K. Wu, E.D. Wang, S. Kamado, G.J. Wang, X.Y. Lv, *Mater. Sci. Eng. A* 547 (2012) 93.
- [8] Y.J. Wu, L.M. Peng, X.Q. Zeng, D.L. Lin, W.J. Ding, Y.H. Peng, *J. Mater. Res.* 24 (2009) 3596.
- [9] Z. Leng, J. Zhang, H. Lin, P. Fei, L. Zhang, S. Liu, M. Zhang, R. Wu, *Mater. Sci. Eng. A* 576 (2013) 202.
- [10] R.B. Figueiredo, T.G. Langdon, *Adv. Eng. Mater.* 10 (2008) 37.
- [11] Q. Yang, B.L. Xiao, Z.Y. Ma, R.S. Chen, *Scripta Mater.* 65 (2011) 335.
- [12] A. Uoya, T. Shibata, K. Higashi, A. Inoue, T. Masumoto, *J. Mater. Res.* 11 (1996) 2731.
- [13] Q. Yang, B.L. Xiao, D. Wang, M.Y. Zheng, K. Wu, Z.Y. Ma, *J. Alloys Compd.* 581 (2013) 585.
- [14] J.W. Edington, K.N. Melton, C.P. Cutler, *Prog. Mater. Sci.* 21 (1976) 61.
- [15] Q. Yang, B.L. Xiao, Z.Y. Ma, *J. Alloys Compd.* 551 (2013) 61.
- [16] M. Yamasaki, M. Sasaki, M. Nishijima, K. Hiraga, Y. Kawamura, *Acta Mater.* 55 (2007) 6798.
- [17] R.B. Figueiredo, T.G. Langdon, *Scripta Mater.* 61 (2009) 84.
- [18] Z.Y. Ma, R.S. Mishra, M.W. Mahoney, R. Grimes, *Metal. Mater. Trans. A* 36A (2005) 1447.
- [19] L. Li, X.M. Zhang, Y.L. Deng, C.P. Tang, *J. Alloys Compd.* 485 (2009) 295.
- [20] W.J. Kim, B.H. Lee, J.B. Lee, M.J. Lee, Y.B. Park, *Scripta Mater.* 63 (2010) 772.
- [21] Y. Miyahara, Z. Horita, T.G. Langdon, *Mater. Sci. Eng. A* 420 (2006) 240.
- [22] F. Chai, D. Zhang, Y. Li, W. Zhang, *Mater. Sci. Eng. A* 568 (2013) 40.
- [23] S.W. Lee, Y.L. Chen, H.Y. Wang, C.F. Yang, J.W. Yeh, *Mater. Sci. Eng. A* 464 (2007) 76.
- [24] M. Furui, H. Kitamura, H. Anada, T.G. Langdon, *Acta Mater.* 55 (2007) 1083.
- [25] H. Watanabe, T. Mukai, K. Ishikawa, T. Mohri, M. Mabuchi, K. Higashi, *Mater. Trans.* 42 (2001) 157.